Steel and Composite Structures, *Vol. 26, No. 2 (2018) 151-161*
DOI: https://doi.org/10.12989/scs.2018.26.2.151

Rehabilitation of notched circular hollow sectional steel beam using CFRP patch

Mahdi Razavi Setvati [a] and Zahiraniza Mustaffa*

Department of Civil and Environmental Engineering, Universiti Teknologi PETRONAS, 32610 Seri Iskandar, Perak, Malaysia

(*Received August 8, 2017, Revised September 29, 2017, Accepted October 21, 2017*)

Abstract. The application of carbon fiber reinforced polymer (CFRP) composites for rehabilitation of steel structures has become vital in recent years. This paper presents an experimental program and a finite element (FE) modelling approach to study the effectiveness of CFRP patch for repair of notch damaged circular hollow sectional (CHS) steel beams. The proposed modeling approach is unique because it takes into account the orthotropic behavior and stacking sequence of composite materials. Parametric study was conducted to investigate the effect of initial damage (i.e., notch depth) on flexural performance of the notched beams and effectiveness of the repair system using the validated FE models. Results demonstrated the ability of CFRP patch to repair notched CHS steel beams, restoring them to their original flexural stiffness and strength. The effect of composite patch repair technique on post-elastic stiffness was more pronounced compared to the elastic stiffness. Composite patch repair becomes more effective when the level of initial damage of beam increases.

Keywords: rehabilitation; circular hollow sectional steel beam; CFRP

1. Introduction

Many steel infrastructures around the world are structurally deficient and need repair (Allan *et al*. 2016). A significant number of oil and gas platforms in the world are approaching or have exceeded their original design life, which was specified as typically 25 years. For instance, 127 fixed offshore platforms on the United Kingdom Continental Shelf (UKCS), approximately 50% of the total platforms, are beyond their original design life. It is evident that this proportion is continuously increasing with time, especially as the rates of platform decommissioning and new installations are fairly low (Stacey and Birkinshaw 2008). Hollow section steel members have widely adopted as structural and nonstructural elements for onshore and offshore structures. In practice, hollow section members are suffering significant deterioration caused by the combination of external loading, corrosion, and cracking (Tao *et al*. 2015). A conventional approach for repair of structurally deficient steel structures is welding or bolting steel plates onto damaged structures (Gholami *et al*. 2016). In the case of the offshore structures, the total cost of a welding repair can be considerably increased because of the need to shut down production during hot works for safety grounds (Allan *et al*. 2016). On the other hand, bolting might not be a desirable alternative because a significant part of the cross sectional area might be lost as a result of drilling for holes (Ragheb 2015). The implement of contemporary materials and repair techniques become essential to resolve these issues (Sundarraja and Ganesh Prabhu 2013).

Previous research has been established carbon fiber reinforced polymer (CFRP) as a promising alternative repair technique for damaged steel structures. It can be used externally to enhance the shear and flexural capacities of beams (Faris and Mehtab 2015). CFRP materials have been used for repair of damaged (i.e., corroded or cracked) I-sectioned steel beams (Allan *et al*. 2016, Tavakkolizadeh and Saadatmanesh 2003, Abdullah *et al*. 2004, Amr and Amir 2008, Amir *et al*. 2009, Yail and Kent 2010, 2011, 2012, Amer *et al*. 2011, Yail and Garrett 2011, Galal *et al*. 2012, Hongyu *et al*. 2013, Jun *et al*. 2016), rectangular hollow sectional (RHS) steel beams (Tao *et al*. 2015, Photiou *et al*. 2006, Mohamed 2014) and circular hollow sectional (CHS) steel beams (Ephrem and Akbar 2012). Moreover, CFRP materials have been used for strengthening intact CHS steel beams (Haedir *et al*. 2009, 2010, 2011, Haedir and Zhao 2012). Ephrem and Akbar (2012) experimentally investigated repair of corroded CHS steel beams using composite wrapping. However, the repair of an existing structure relies mostly on the available access for repair (Mohamed 2014) and in some cases it could be difficult to fully wrap the CHS beams by composite, especially when these beams used in the floor system or as a bridge's girder because the loads are applied on the top surface of the beams. In view of the reported literatures, it could be seen that there is limited attention to repair of damaged CHS steel beams and, therefore, this research gap should be fulfilled. Furthermore, most results in the existing literature are based on experimental observations and very limited knowledge is available from a modeling viewpoint (Yail and Kent 2012).

This paper presents an experimental program and

*Corresponding author, Associate Professor,
E-mail: zahiraniza@utp.edu.my
[a] Ph.D. Scholar, E-mail: m.razavis_g02622@utp.edu.my

ISSN: 1229-9367 (Print), 1598-6233 (Online)

proposes a finite element (FE) modelling approach to investigate the effectiveness of CFRP patch for repair of notch damaged CHS steel beams. The proposed modeling approach is unique because it takes into account the orthotropic behavior and stacking sequence of composite materials. Parametric study was conducted to investigate the effect of initial damage (i.e., notch depth) on flexural behavior of the notched beams and effectiveness of the repair system using the validated FE models.

2. Experimental program

An experimental program was carried out to study the flexural behavior of undamaged (intact), notched and CFRP patch repaired CHS steel beams. Moreover, experimental results were also utilized to validate the corresponded FE models. This section describes the properties of materials, details of experimental specimens, test setup and instrumentation.

2.1 Materials

2.1.1 Steel

Three 1170-mm-long CHS steel beams were used in this study. The yield, tensile strengths and Young's modulus of the steel were 264 MPa, 450 MPa and 200 GPa, respectively.

2.1.2 CFRP laminates

The carbon fiber fabric Sikawrap -231C and the epoxy impregnation resin Sikadur -330 were utilized as the repair materials. The Sikawrap and the Sikadur were chosen due to its wide structural applications (Jun and Marcus 2007). It is worth noting that Ahmed *et al*. (2017) utilized exactly same materials (Sikawrap -231C and Sikadur -330) for repair of concrete-filled steel tubular (CFST) beams. The Sikawrap -231 is a unidirectional carbon fiber fabric with high strength having a nominal thickness of 0.13 mm/ply and Sikadur -330 is a two-part, thixotropic epoxy based impregnating resin/adhesive. The epoxy adhesive consisting of Part A (resin) and Part B (hardener). The Sikawrap -231 (having strength of 4900 MPa, stiffness of 230 GPa, and maximum strain of 2.1%) and Sikadur -330 (having tensile strength of 30 N/mm^2, flexural E- modulus of 3800 N/mm^2 and tensile E-modulus of 4500 N/mm^2 (7 days at +23°C)) constitute CFRP composite with thickness of 1 mm, as per the manufacturer specifications. Tables 1 and 2 summarize material properties of Sikawrap -231C and Sikadur -330, respectively.

Table 1 Properties of Sikawrap -231C

Strength	Stiffness	Maximum strain
4900 MPa	230 GPa	2.1%

Table 2 Properties of Sikadur -330

Tensile strength	Flexural E-modulus	Tensile E-modulus
30 N/mm^2	3800 N/mm^2	4500 N/mm^2

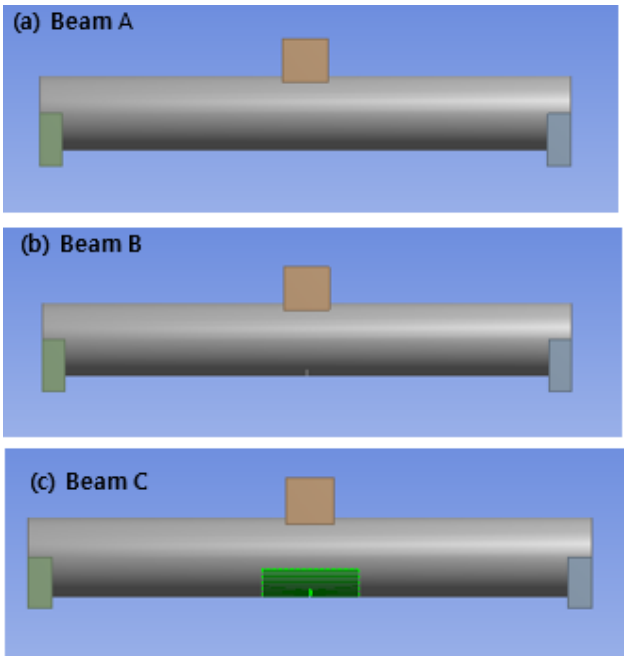

Fig. 1 CHS beams: (a) Undamaged beam (Beam A); (b) Notched beam (Beam B), (c) Repaired notched beam

Table 3 Dimensions of CHS steel beam

Length	External diameter	Thickness
1170 mm	168.3 mm	14.3 mm

2.2 Beam details

Three CHS steel beams, including one undamaged control beam (Beam A), one notched beam (Beam B), and one repaired notched beam (Beam C), as shown in Fig. 1, were studied. Dimensions of CHS beam are given in Table 3. The specimen preparation involved notch creation, surface preparation, and applying wet lay-up CFRP.

2.2.1 Notch creation

Amir *et al*. (2009), Amer *et al*. (2011), Tao *et al*. (2015), and Ahmed *et al*. (2017) created notches on bottom surface of steel beams to simulate crack damage in beams. In this study, 14.3 mm-deep notches (Fig. 2) were created at mid-span of two CHS beams using 3 mm-thick band-saw to represent crack damage, following the same crack-simulation technique adopted in the above-mentioned literatures.

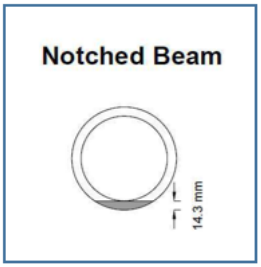

Fig. 2 Details of notch damage

2.2.2 Surface preparation

Although proper surface preparation of steel substrate is an important step to achieve a good bond joint between the steel and CFRP (Mohamed 2014, Ephrem and Akbar 2012, Akbar *et al*. 2010), specific requirements have not been developed yet (Amir *et al*. 2009). In this study the bottom surfaces of Beam C was roughened with an electric grinder to enhance bond between the steel and composite material. It should be noted that similar procedure was adopted by Yail and Garrett (2011) and Ahmed *et al*. (2017) for surface preparation. The surface of the samples were thoroughly cleaned with mechanical brush and acetone immediately prior to the application of composite repair. This was done to ensure that the surface was clean from any of the contaminants such as dust and rust.

2.2.3 CFRP patch repair

The design of structures with fiber composites is mostly governed by stiffness rather than strength (Allan *et al*. 2016). The damaged portion of the CHS beam is replaced with an equivalent area of CFRP patch to keep the overall stiffness of the beam unchanged. The cross-sectional area of CFRP required, A_{CFRP}, was estimated using the following equation

$$A_{CFRP} = \frac{E_s}{E_{CFRP}} A_{S(removed\ )} \quad (1)$$

Where E_s is Young's modulus of steel, E_{CFRP} is Young's modulus of CFRP and $A_{S(removed\ )}$ is the steel cross-sectional area removed by cutting the notch.

The misfit in deformations between the steel beam and composite laminate leads to concentrations of both peel stress (σ) and shear stress (τ) across the adhesive joint (Hollaway and Teng 2008). If the bonded repair is subjected to a load that exceeds its resistance, a brittle debonding fracture occurs. Maeda *et al*. (1997) proposed an empirical equation to calculate effective bond length for a FRP sheet bonded to a concrete surface. This equation is currently in use in the ACI 440.2R-08 and CAN/CSA S6-06 design guidelines (Amir and Omar 2011). For steel application, DNV-RP-C301 stated that stress approach underrated the bondline capacity of patch repair by a factor ranging from 2 to 6 for different choices of patch materials and geometry. A dedicated experimental study on the bonded repair showed that the strain at fracture is not a suitable measure of failure (DNV-RP-C301). Whilst fracture mechanics approaches are used to design adhesive joints in the aerospace industry, they have yet to be developed for civil engineering purposes (Hollaway and Teng 2008). In particular, aerospace applications use much thinner repair materials, in which peel stresses are low. The mixed mode (peel–shear) behavior in typical civil engineering applications has not yet been reliably characterised using the fracture mechanics techniques (Hollaway and Teng 2008). It has proven difficult to develop reliable fracture mechanics criteria where the fracture resistance parameters are established from idealized material tests and then used in a general model to predict failure of realistic repair configurations (DNV-RP-C301). Therefore, in this study the CFRP patch repairs were sized by trial-and-error method using the developed finite element model (FEM) in order to enable the CFRP repair to restore the full flexural stiffness and strength of the damaged beam. The developed FEM includes cohesive zone technology which models contact debonding failure. The cohesive zone allows normal, tangential and mixed mode (peel–shear) separation, as discussed further in Subsection 3.3.3. One notch beam was repaired by a 14 mm-thick (14-ply), 20 × 21 cm CFRP patch, as shown in Fig. 3. It should be noted that a large number of composite layers is common in the composite repair industry as Allan *et al*. (2016) used 15-ply composite, Karatzas *et al*. (2013) utilized 16-ply composite and Tsouvalis *et al*. (2008) used 18-ply composite for repair purpose.

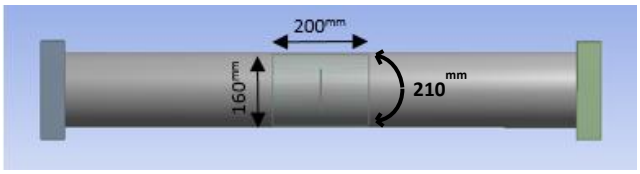

Fig. 3 Dimensions of CFRP patch repair

The carbon fiber sheets were applied underneath the notched sample using saturating epoxy as both a resin and adhesive in a wet lay-up (hand lay-up) system. The 0.13 mm-thick carbon fiber fabrics (Sikawrap -231C) were cut to the sizes using scissors. The mixing ratio of Sikadur -330 part A to part B is 4:1 by weight, respectively. The mixing procedure of part A and part B is given as follows:

i. The materials in each container were stirred separately.
ii. Part A was added to part B using the special Sika spatula.
iii. The solution was mixed for approximately three minutes until all color streaks disappeared.

The whole mix was poured into a clean container and stirred again for roughly one minute at low speed to avoid air being tapped in the mixture.

After the carbon fiber fabric was properly saturated with the adhesive, it was installed on the notched beam manually while keeping the center of the patch with the center of the damage. First ply aligned with the longitudinal direction of the beam, while the second ply positioned at 90° to the longitudinal direction of sample, and this procedure was continued to the last ply (i.e., fiber orientations of odd plies are parallel to longitudinal direction of the beams, whereas fiber orientations of even plies are perpendicular to longitudinal direction of samples). Each layer was rolled onto the steel surface to remove any air bubbles. The composite repair was left to cure for a minimum of one week in the laboratory prior to experimental testing.

2.3 Test setup and instrumentation

The specimens were subjected to three-point bending under static load conditions, as shown in Fig. 4. Such a testing scheme is particularly useful for studying the performance of damaged beams (Yail and Garrett 2011). One linear variable differential transformer (LVDT) was located at mid span (immediately beneath the applied load)

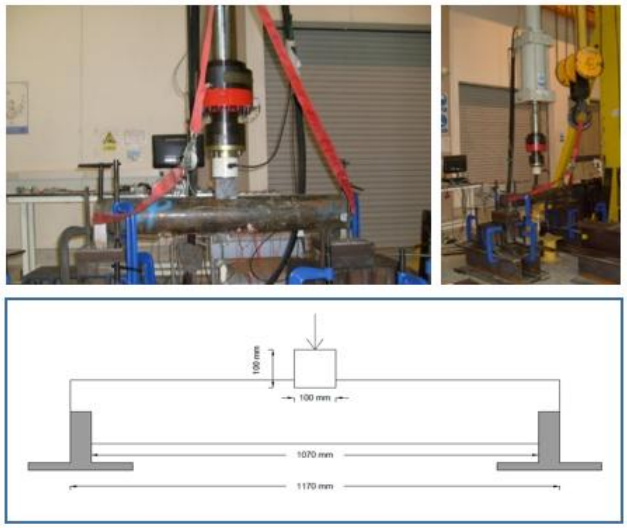

Fig. 4 Three-point bending test

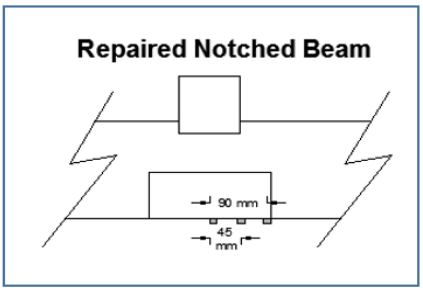

Fig. 5 Positions of strain gauges on repaired beam

to measure the deflection of the sample. Three KYOWA, 2-mm-long, strain gauges were mounted on the surface of the CFRP patch to measure longitudinal strains of the composite repair. Fig. 5 shows the positions of the strain gauges on the experimental samples. The load, midspan deflection, and strains at different points were recorded with a data acquisition system.

3. Proposed model

Numerical simulations have been used as complementary and cost-effective methods to experiments, as the latter could be time consuming and limited in its scope to cover extensive testing parameters (Chao *et al.* 2012). This section summarizes a modelling approach to predict the performance of notched CHS steel beam repaired by CFRP patch when subjected to static loading. The FEA program ANSYS Workbench (Version 15) and ANSYS Composite PrepPost (ACP) module were used. ACP is an add-on module to ANSYS software dedicated to modelling layered composite structure.

3.1 Mesh

The geometrical models were meshed into elements, as shown in Fig. 6, using combination of the auto meshing and map meshing in order to achieve the best solution. It should

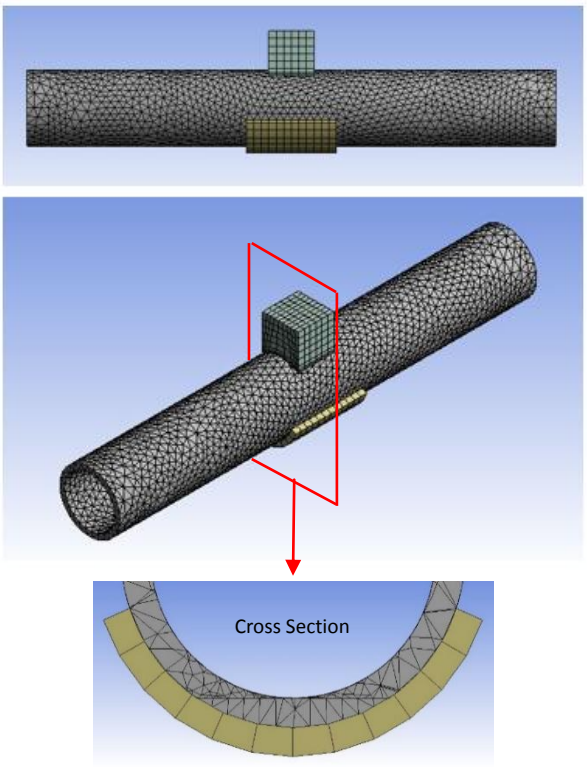

Fig. 6 Constructed FE model

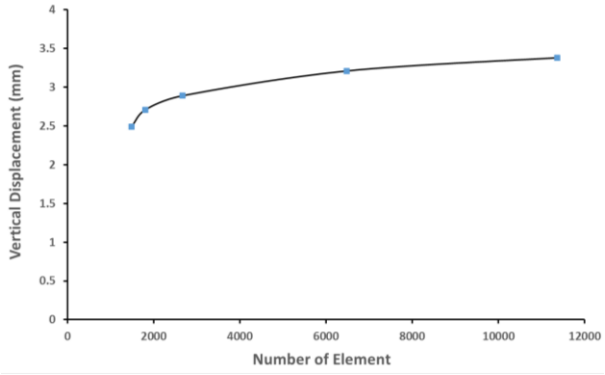

Fig. 7 Mesh convergence study

be noted that Kambiz *et al.* (2012) implemented the same method for meshing their finite element models and they achieved very accurate results. A relatively fine mesh was used based on the results of mesh convergence study, as shown in Fig. 7.

3.2 Element description

The CHS steel beams were modeled with 3-D, higher order SOLID187 element. This element has a quadratic displacement behavior and is well suited for irregular mesh, such as that produced near damaged region. It should be noted that Hui-Huan *et al.* (2015) used SOLID187 for modelling tubular steel member and bolted-plate steel connections. SHELL181 elements were used to represent CFRP patch repair. Shell elements generally have a unique quality of easy convergence during simulation (Agbomerie

et al. 2017). SHELL181 can be used for layered applications for modeling composite shells or sandwich construction (ANSYS Inc. 2015). It should be noted that Pouria *et al*. (2015) employed SHELL181 for modelling composite layers (laminates). SOLID187 and SHELL188 are current-technology elements (sometimes called new-generation elements). The current element type uses more advanced technologies rather than legacy elements (ANSYS Inc 2015). The interfacial behavior between composite and steel was modeled using CONTA174 and TARGE170 elements. CONTA174 is used to represent contact and sliding between 3-D "target" surfaces (TARGE170) and a deformable surface, defined by this element. It should be noted that Burlović *et al*. (2016) also used CONTA174 and TARGE170 for modelling interface between composite and steel.

3.3 Material properties and constitutive models

The material modeling of steel, composite and adhesive is an important part in the numerical analysis and should be done carefully to represent the actual behavior of FE models, as explained in the following subsections:

3.3.1 Steel

While engineering stress strain curve can be used for small strain analysis, true stress strain must be used for plasticity, as they are more representative measures of the state of material (ANSYS Inc. 2014). It should be noted that Fernando *et al*. (2009) and Fernando *et al*. (2015), who studied CFRP-strengthened rectangular steel tubes, used true strain stress curve for their finite element analysis. The steel non-linearity (plasticity) was accounted for in the model by specifying a bi-linear isotropic hardening model, as shown in Fig. 8. The bilinear isotropic hardening model was used in many numerical studies. For instance, Iftekharul and Sabrina (2015) used this hardening model in the finite element analysis of CFRP strengthened steel CHS column. The tangent modulus set as 2000 MPa in compliance with Eurocode 3.

3.3.2 CFRP

An orthotropic material has three planes of symmetry that coincide with the coordinate planes. A unidirectional fiber reinforced composite may be considered to be orthotropic. One plane of symmetry is perpendicular to the fiber direction, and the other two are orthogonal to the fiber direction and among themselves (Ever 2013). The CFRP patch materials in this study were defined as orthotropic and linear (Fig. 9) because used CFRP materials were unidirectional and they have linear properties (Yail and Kent 2011, Yail and Garrett 2011, Linghoff *et al*. 2009, Kambiz *et al*. 2012). Material properties of CFRP laminate obtained from manufacturer were implemented in the current model, as shown in Fig. 10.

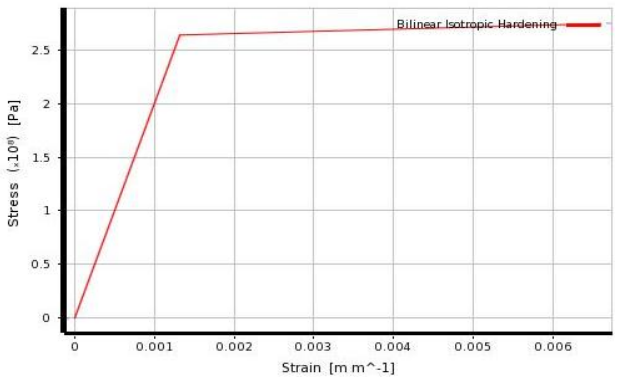

Fig. 8 Bi-linear isotropic hardening model of steel

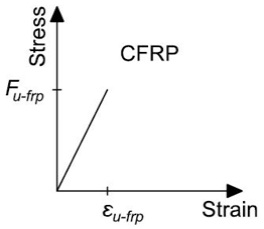

Fig. 9 Constitutive model of CFRP

Properties of Outline Row 4: Epoxy_Carbon_UD_230GPa_Wet

	A	B	C
1	Property	Value	Unit
9	Orthotropic Elasticity		
10	Young's Modulus X direction	1.2334E+05	MPa
11	Young's Modulus Y direction	7780	MPa
12	Young's Modulus Z direction	7780	MPa
13	Poisson's Ratio XY	0.27	
14	Poisson's Ratio YZ	0.42	
15	Poisson's Ratio XZ	0.27	
16	Shear Modulus XY	5000	MPa
17	Shear Modulus YZ	3080	MPa
18	Shear Modulus XZ	5000	MPa

Fig. 10 Material properties of CFRP

3.3.3 Adhesive

Several researchers, such as Burlović *et al*. (2016), Teng *et al*. (2015), Fernando *et al*. (2015), Kotsidis *et al*. (2014) and Anyfantis (2012) have implemented Cohesive Zone Model (CZM) for modelling the adhesively bond between composite and metal and they have achieved very accurate results as in their related experimental results. The CZM is based on the concepts of stress and fracture mechanics, and can be fitted into the local or continuum approach (Silva *et al*. 2012). It is capable of simulating the damage initiation and growth (Karatzas *et al*. 2013). This approach introduces a failure mechanisms by gradually degrading the material elasticity between the surfaces. The material behavior at the interface is characterized by the stresses (normal and tangential) and separation distances (normal gap and tangential sliding) (CAE Associates 2012). The CZM is based on traction-separation constitutive law. Several shapes for the traction-separation law exist in the literature as follow: the bilinear, linear-parabolic, exponential and trapezoidal shapes. The bilinear law (Fig. 11) is well suited for the modeling of resins and non-ductile adhesives

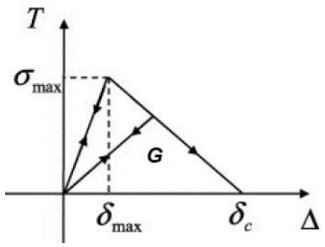

Fig. 11 The bilinear traction separation law (Karatzas *et al*. 2013)

Table 4 Traction-separation parameters for Sikadur-330 adhesive

Loading mode	Maximum stress (MPa)	Critical fracture energy (N/mm)
Mode I	31.28	0.106
Mode II	28.15	7.056

(Karatzas *et al*. 2013).

The material properties required for the cohesive law are:

i. Maximum normal stress
ii. Maximum tangential stress
iii. Critical fracture energy for normal separation (mode I)
iv. Critical fracture energy for tangential slip (mode II)

In this study the CZM was used to model adhesive between composite and steel and CZM parameters were taken from Fernando *et al*. (2015), as summarized in Table 4. Fernando *et al*. (2015) calculated CZM parameters for the Sikadur-330 adhesive based on the approach which were proposed by Teng *et al*. (2015), Fernando (2010) and Campilho *et al*. (2008).

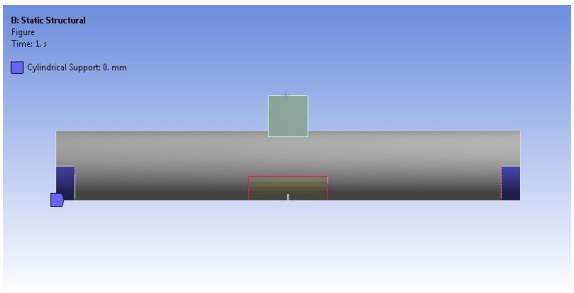

Fig. 12 Cylindrical supports of CHS beam

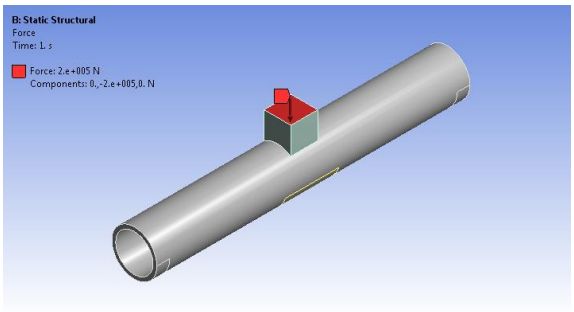

Fig. 13 Applied load in vertical direction

3.4 Boundary conditions and loading

The cylindrical supports were assigned at two ends of the beams due to the curved surface of the CHS beam, as shown in Fig. 12. The tangential movement was set into fixed while axial and radial movements were defined as free to keep the boundary conditions consistent with the experiments. The Bonded contact was defined between the top surface of the steel beam and the bottom surface of the block which transfers the applied load. This Bonded contact fixes the surfaces to one another, so sliding or separation cannot occur. The load in the vertical direction at mid-span of the beam on a certain area corresponding to the load application region in the experimental tests was applied, as shown in Fig. 13.

3.5 Validation

The validation of FE approach was achieved in two steps. Firstly, the load-deflection curves of the three aforementioned beams obtained by computational simulation were compared with counterpart experimental results. Secondly, predicted strain distributions in the composite patch of Beam C were compared with the corresponding strains measured by the strain gauges.

4. Results

This section provides and discusses experimental and predicted results of the study, including load-deflection responses of three CHS steel beams, strain analysis of CFRP patch, and effects of notch depth (level of initial damage) on the flexural performance of the notched CHS steel beam and effectiveness of the CFRP patch repair.

4.1 Load-displacement response

Figs. 14 to 16 show the midspan load-displacement responses of the predicted and experimental Beams A (intact beam), B (notched beam) and C (repaired notched

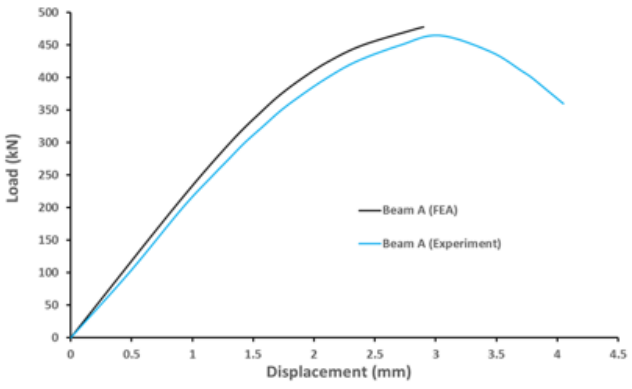

Fig. 14 Load-displacement response of undamaged beam (Beam A)

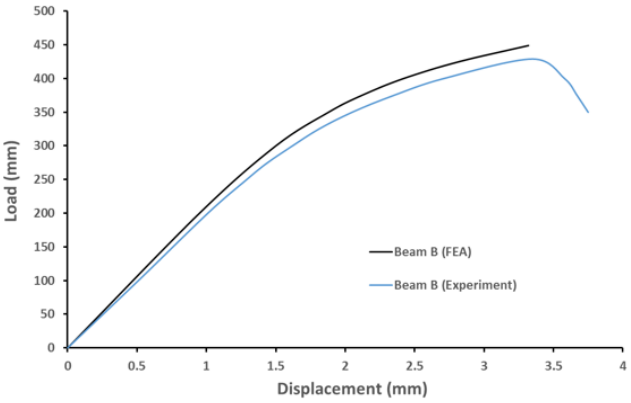

Fig. 15 Load-displacement response of notched beam (Beam B)

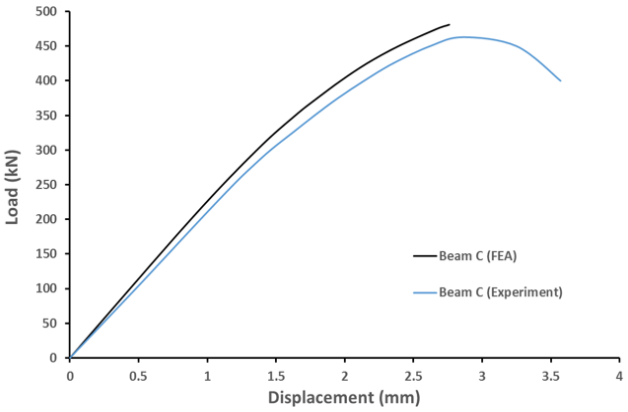

Fig. 16 Load-displacement response of repaired beam (Beam C)

beam), respectively. These figures indicate that the predicted load-displacement response agreed well with that measured experimentally with an average error of 7.8%. Experimental uncertainty, such as thickness of adhesive in a wet layup application, and assumptions in FEA, such as bilinear model of steel, could have contributed to the discrepancy. The load–displacement curves became nonlinear, mainly because of the steel plasticity, following a linear elastic range. The unrepaired beams failed by yielding of steel section, whereas the repaired beam failed due to the rupture of CFRP patch (i.e., patch fracture). Similar failure modes were reported for repaired I-sectioned beams under three-point bending by Hongyu *et al*. (2013). Gradual load-softening was observed beyond the ultimate load of the experimental beams.

Fig. 17 compared load-displacement curves of computational Beams A, B and C. A summary of the predicted elastic stiffness and strength of the beams is given in Table 5. It can be observed that repaired notched beam (Beam C) exhibited an increase in stiffness as well as ultimate strength, compared to the notched beam (Beam B). The load-sharing mechanism between the steel and CFRP improved the flexural capacity of the repaired beams. The repair effect was more pronounced in the post-elastic region compared to the elastic region. This finding is consistent

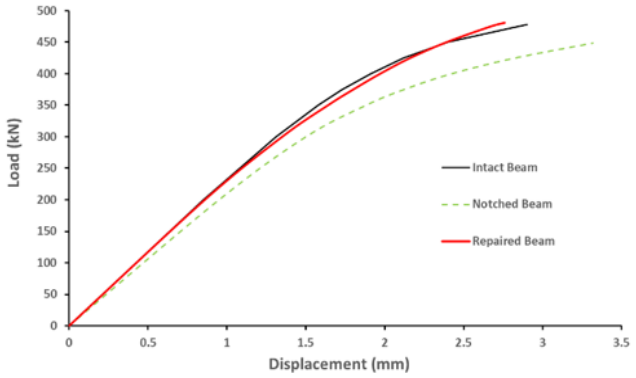

Fig. 17 Comparison of predicted results

Table 5 Predicted results of the beams

Beam identification	Elastic stiffness (kN/mm)	Strength (kN)
Beam A	224	478
Beam B	206	449
Beam C	226	481

with observations from other studies by Ahmed *et al*. (2017) and Ahmed *et al*. (2015), who conducted researches on the composite repaired CFST beams. This finding can be explained by the fact that following yield, and the loss of stiffness of the steel, the contribution of the CFRP repair becomes greater. The elastic stiffness of notched beam (Beam B) and repaired notched beam (Beam C) are 206 and 226 kN/mm, respectively, which are 92 and 100.9% of that of undamaged beam (224 kN/mm). The flexural strength of notched beam and repaired notched beam are 449 and 481 kN, respectively, which are 93.9 and 100.6% of that of undamaged beam (478 kN). Therefore, the notch damage reduced elastic stiffness and flexural strength of the undamaged beam by 8 and 6.1%, respectively, and composite repair recovered 8.9 and 6.7% of those, respectively, compared to undamaged beam. These results demonstrated the ability of CFRP patch repair to restore full bending capacity of the notched CHS steel beam.

4.2 Strain distributions in CFRP patch

The longitudinal strain distributions in the composite

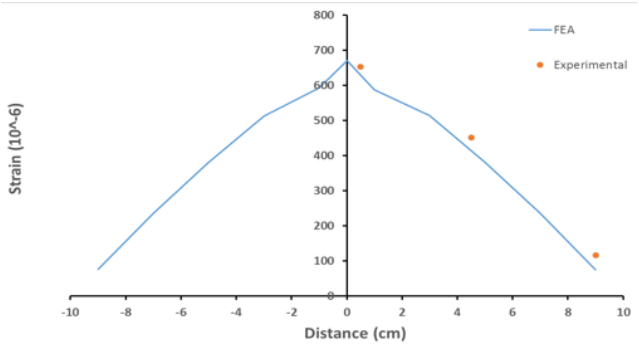

Fig. 18 Longitudinal strain distributions in CFRP patch of Beam C

patch of the repaired notched beam (Beam C) at a load of 50% P_u (typical service state) was graphed in Fig. 18. The computed strains agreed well with those measured experimentally.

A symmetrical non-uniformly distribution shape was observed. The longitudinal strain at mid-span achieved the maximum value because the geometrical discontinuity at notched region caused stress concentration at mid-span of the beam. The strain value significantly decreased away from mid-span to two terminations of the CFRP patch. It is worth noting that Tao *et al*. (2015) reported that strains distribute non-uniformly in CFRP plate for nonprestressed specimen, and strains distribute uniformly in CFRP plate for prestressed specimen. Moreover, Tao *et al*. (2015) indicated that prestressed CFRP plate utilization efficiency is better than nonprestressed one due to prevention of strain concentration at prestressed composite plate.

4.3 Parametric study

A parametric finite element study was carried out to examine the effect of level of initial damage (i.e., notch depth) on the flexural behavior of the notched beams and effectiveness of CFRP patch repair. Three notch depths of 14.3 (equal to beam thickness), 28.6 (equal to twice beam thickness) and 42.9 mm (equal to three times beam thickness) were considered to represent different levels of initial damage.

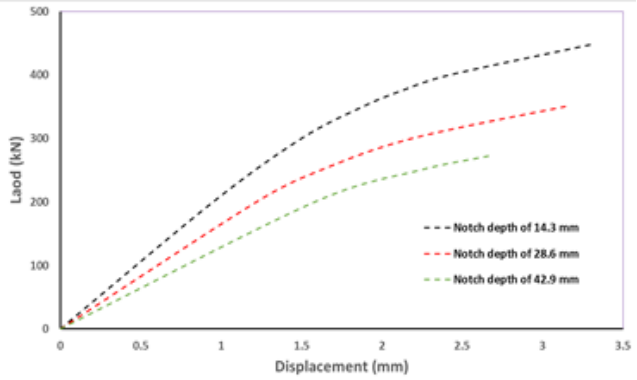

Fig. 19 Load-Displacement of beams having three notch depth of 14.3, 28.6 and 42.9 mm

Table 6 Summary of stiffness and strength of notched beams

Beams	Elastic stiffness (kN/mm)	Strength (kN)
Beam having notch depth of 14.3 mm	206	449
Beam having notch depth of 28.6 mm	163	351
Beam having notch depth of 42.9 mm	126	273

Table 7 Summary of stiffness and strength of repaired beams

Beams	Elastic stiffness (kN/mm)	Strength (kN)
Repaired beam having notch depth of 14.3 mm	226	481
Repaired beam having notch depth of 28.6 mm	217	395
Repaired beam having notch depth of 42.9 mm	213	318

4.3.1 Effect of level of initial damage on notched beam

Fig. 19 shows the predicted load-displacement response at midspan of the beams having different three notch depths and Table 6 provides a summary of the elastic stiffness and strength of the beams. It can be seen that the notched beams experienced linear behavior at the beginning of the loading, and the load-displacement curves soon became nonlinear after a short elastic regime. Since the underneath of the CHS beams at midspan were notched and could no longer transfer stress, the nonlinearity of the load-displacement response were primarily caused by the steel plasticity near notch location. The beams failed by yielding of steel sections. The elastic stiffness and strength of notched beams decreased as initial damage increased. For instance, the stiffness of the notched beams having notch depths of 14.3, 28.6, and 42.9 mm were 206, 163, and 126 kN/mm, respectively, which are 92, 72.8 and 56.3% of that of undamaged beam. This is mainly because the moment of inertia of the notched cross section varied substantially with the notch depth. This observation is consistent with the findings of Amer *et al*. (2011) and Yail and Garrett (2011).

4.3.1 Effect of level of initial damage on effectiveness of CFRP patch repair

Beams having different notch depths were repaired by an identical composite patch configuration, 14-ply CFRP of 20 × 21 cm. Fig. 20 illustrates the predicted load-deflection response at midspan of unrepaired and repaired beams. A summary of the predicted elastic stiffness and strength of the beams is given in Table 7. The stiffness and strength of the notched beams were improved because of the composite repair, particularly noticeable when the notch depth (level of damage) increased, as shown in Fig. 20 and Table 7. For example, the increases in strength induced by the composite repair were 7.1, 12.5, and 16.4% for the beams having notch depths of 14.3, 28.6, and 42.9 mm, respectively. These observations demonstrated that composite repair becomes more effective when the level of initial damage increases. This is because the greater initial damage leads to sooner yielding and loss of the stiffness of the steel beam, and, therefore, increasing the contribution of CFRP in load bearing. This result is in line with observations from other studies by Amer *et al*. (2011) and Yail and Garrett (2011).

Failure analyses of composites are significantly more complex than for isotropic materials due to their orthotropic material behavior and multiple possible failure modes (Setvati *et al*. 2016). There are many failure criteria for composite materials, some have been formulated in a general way while others are formulated for specific composites. The following failure criteria are currently available in ACP (V.15): maximum strain, maximum stress, Tsai-Wu, Tsai-Hill, Puck, Hashin, LaRC, Cuntze, Core Failure and Face Sheet Wrinkling (ANSYS Inc. 2014). The failures of CFRP patch repairs were evaluated and

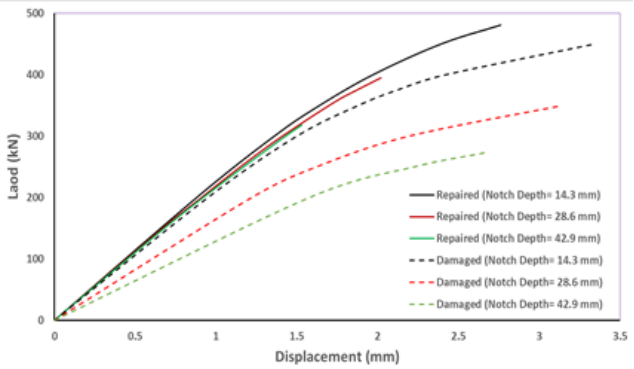

Fig. 20 Load-Displacement of beams having three notch depth of 14.3, 28.6 and 42.9 mm

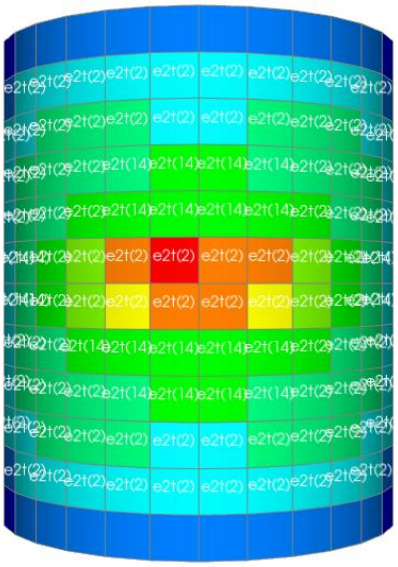

Fig. 21 Result of failure analysis of CFRP patch

visualized in ACP-Post module of ACP as shown in Fig. 21. The failure analysis indicated the three beams failed by the rupture of CFRP patch. Analysis of the beams was stopped as the rupture of CFRP commenced. The critical failure criteria of the repaired beams are maximum strains in the longitudinal direction of the CHS beam. The critical region is the center of the patch, which is close to the notched area of the steel beam, because of strain concentration at this position, which resulting from large deformation of the steel beam at this position.

5. Conclusions

This paper has presented experimental and numerical investigations into the flexural behavior of the CFRP patch repaired notched CHS steel beam. Based on the measured and predicted results, the following is concluded:

i. Results of this study demonstrated the ability of CFRP patch to repair notched CHS steel beams, restoring them to their original flexural stiffness and strength.
ii. The effect of composite patch repair technique on post-elastic stiffness was more pronounced compared to the elastic stiffness.
iii. The proposed FE modelling approach can provide accurate predictions for load-deflection curves of the CFRP patch repaired notched beam and strain distributions of CFRP patch.
iv. A non-uniformly strain distribution in CFRP patch indicted the presence of stress concentration at deficient area of the beam, reducing the efficiency of CFRP patch compared to prestressed CFRP plate, which has uniform strain distribution.

Composite patch repair becomes more effective when the level of initial damage of beam increases.

Acknowledgments

The first author would like to thank for the graduate assistantship of the Universiti Teknologi PETRONAS (UTP) and authors acknowledge University Research Internal Fund (No. 153AA-B74) of UTP. Technical discussions with Prof. Dr. Nasir Shafiq of UTP, Dr. K.H. Leong of PETRONAS Research Sdn Bhd (PRSB), Engr. Biramarta Isnadi of PETRONAS Carigali Sdn Bhd (PCSB), and Dr. Zubair Imam Syed of Abu Dhabi University during this study project have been immensely useful and are gratefully acknowledged.

References

Abdullah, H.A., Klaiber, F.W. and Wipf, T.J. (2004), "Repair of Steel Composite Beams with Carbon Fiber-Reinforced Polymer Plates", *J. Compos. Construct.*, **8**(2), 163-172.

Agbomerie, C.O., Stephen, Q. and Jianqiao, Y. (2017), "Wave induced stress profile on a paired column semisubmersible hull formation for column reinforcement", *J. Eng. Struct.*, **143**, 77-90.

Ahmed, W.A.Z., Wan, H.W.B., Azrul, A.M. and Qahtan, A.H. (2015), "Finite element analysis of square CFST beam strengthened by CFRP composite material", *J. Thin-Wall. Struct.*, **96**, 348-358.

Ahmed, W.A.Z., Wan, H.W.B., Azrul, A.M. and Salam, J.H. (2017), "Rehabilitation and strengthening of high-strength rectangular CFST beams using a partial wrapping scheme of CFRP sheets: Experimental and numerical study", *J. Thin-Wall. Struct.*, **114**, 80-91.

Akbar, I., Oehlers, D.J. and MohamedAli, M.S. (2010), "Derivation of the bond–slip characteristics for FRP plated steel members", *J. Construct. Steel Res.*, **66**(8), 1047-1056.

Allan, M., Chamila, S., Warna, K., Lance, M.G. and Paul, F. (2016), "Pre-impregnated carbon fibre reinforced composite system for patch repair of steel I-beams", *J. Construct. Build. Mater.*, **105**, 365-376.

Amer, H. (2014), "Crack-Dependent Response of Structural Steel Members Repaired with CFRP", Ph.D. Thesis; North Dakota State University, USA.

Amer, H., Yail, J.K. and Siamak, Y. (2011), "CFRP Repair of Steel Beams with Various Initial Crack Configurations", *J. Compos. Construct.*, **15**(6), 952-962.

Amer, H., Yail, J.K. and Siamak, Y. (2013), "Crack-dependent response of steel elements strengthened with CFRP sheets", *J. Construct. Build. Mater.*, **49**, 110-120.
American Concrete Institute (ACI) (2008), "Guide for the design and construction of externally bonded FRP systems for strengthening concrete structures", *Rep. No. 440 2R-08*, Farmington Hills, MI, USA.
Amir, F., Colin, M.D. and Amr, S. (2009), "Upgrading steel–concrete composite girders and repair of damaged steel beams using bonded CFRP laminates", *J. Thin-Walled Struct.*, **47**(10), 1122-1135.
Amr, S. and Amir, F. (2008), "Repair of cracked steel girders connected to concrete slabs using carbon-fiber-reinforced polymer sheets", *J. Compos. Construct.*, **12**(6), 650-659.
Amir, M. and Omar, C. (2011), "Shear strengthening of RC beams with EB FRP: Influencing factors and conceptual debonding model", *J. Compos. Construct.*, **15**(1), 62-74.
ANSYS Inc. (2014), ANSYS Composite PrepPost (ACP) Training, Available at: https://support.ansys.com/AnsysCustomerPortal/en_us
ANSYS Inc. (2015), ANSYS Mechanical APDL Element Reference (V.15), Available at: http://148.204.81.206/Ansys/150/ANSYS%20Mechanical%20APDL%20Element%20Reference.pdf
Anyfantis, K.N. (2012), "Finite element predictions of composite-to-metal bonded joints with ductile adhesive materials", *J. Compos. Struct.*, **94**(8), 2632-2639.
Burlović, D., Milat, A., Balunović, M., Frank, D., Kotsidis, E.A., Kouloukouras, I.G. and Tsouvalis, N.G. (2016), "Finite element analysis of composite-to-steel type of joint for marine industry", *Weld. World*, **60**(5), 859-867.
CAE Associates (2012), ANSYS Cohesive Zone Modeling; Website of CAE Associates. (https://caeai.com/ansys-training)
Campilho, R.D.S.G., Moura, M.F.S.F. and Domingues, J.J.M.S. (2008), "Using a cohesive damage model to predict the tensile behaviour of CFRP single-strap repairs", *Int. J. Solids Struct.*, **45**(5), 1497-1512.
CAN/CSA (2006), Canadian highway bridge design code; S6-06, Canadian Standards Association, Mississauga, Canada.
Chao, W., Xiaoling, Z., Wen, H.D. and Riadh, A. (2012), "Bond characteristics between ultra-high modulus CFRP laminates and steel", *J. Thin-Wall. Struct.*, **51**, 147-157.
DNV-RP-C301 (2012), Design, Fabrication, Operation and Qualification of Bonded Repair of Steel Structures; Det Norske Veritas.
Ephrem, A. and Akbar, I. (2012), "The flexural behaviour of tubular steel member strengthened with CFRP", *The Proceedings of 8th Asia Pacific Structural Engineering and Construction Conference and 1st International Conference for Civil Engineering Research*, Surabaya, Indonesia, October.
Eurocode3 (2005), Design of Steel Structures—Parts 1–8: Design of Joints (BSEN 1993-1-8:2005), Standards Policy and Strategy Committee.
Ever, J.B. (2013), *Finite Element Analysis of Composite Materials using ANSYS*, (2nd Ed.), CRC Press, ISBN: 9781466516892.
Faris, A.U. and Mehtab, A. (2015), "Steel–CFRP composite and their shear response as vertical stirrup in beams", *Steel Compos. Struct., Int. J.*, **18**(5), 1145-1160.
Fernando, D. (2010), "Bond behaviour and debonding failures in CFRP-strengthened steel structures", Ph.D. Thesis; Department of Civil and Structural Engineering, Hong Kong Polytechnic University, Hong Kong, China.
Fernando, D., Yu, T., Teng, J.G. and Zhao, X.L. (2009), "CFRP strengthening of rectangular steel tubes subjected to end bearing loads: Effect of adhesive properties and finite element modelling", *J. Thin-Wall. Struct.*, **47**(10), 1020-1028.
Fernando, D., Yu, T. and Teng, J.G., (2015), "Behavior and modeling of CFRP-strengthened rectangular steel Tubes subjected to a transverse end bearing load", *Int. J. Struct. Stabil. Dyn.*, **15**(8).
Galal, K., Seif ElDin, H.M. and Tirca, L. (2012), "Flexural Performance of Steel Girders Retrofitted Using CFRP Materials", *J. Compos. Construct.*, **16**(3), 265-276.
Gholami, M., Mohd Sam, A.R., Marsono, A.K., Tahir, M.M. and Faridmehr, I. (2016), "Performance of steel beams strengthened with pultruded CFRP plate under various exposures", *Steel Compos. Struct., Int. J.*, **20**(5), 999-1022.
Haedir, J. and Zhao, X.L. (2012), "Design of CFRP-strengthened steel CHS tubular beams", *J. Construct. Steel Res.*, **72**, 203-218.
Haedir, J., Bambach, M.R., Zhao, X.L. and Grzebieta, R.H. (2009), "Strength of circular hollow sections (CHS) tubular beams externally reinforced by carbon FRP sheets in pure bending", *J. Thin-Wall. Struct.*, **47**(10), 1136-1114.
Haedir, J., Zhao, X.L., Bambach, M.R. and Grzebieta, R.H. (2010), "Analysis of CFRP externally-reinforced steel CHS tubular beams", *J. Compos. Struct.*, **92**(12), 2992-3001.
Haedir, J., Zhao, X.L., Grzebieta, R.H. and Bambach, M. (2011), "Non-linear analysis to predict the moment–curvature response of CFRP-strengthened steel CHS tubular beams", *J. Thin-Wall. Struct.*, **49**(8), 997-1006.
Hollaway, L.C. and Teng, J.G. (2008), *Strengthening and rehabilitation of civil infrastructures using fibre-reinforced polymer (FRP) composites*, Woodhead Publishing and Maney Publishing.
Hongyu, Z., Thomas, L.A., Yanli, W., Jy-An, W. and Fei, R. (2013), "Rehabilitation of notch damaged steel beams using a carbon fiber reinforced hybrid polymeric-matrix composite", *J. Compos. Struct.*, **106,** 690-702.
Hui-Huan, M., Ali, M.I., Feng, F. and Guy, O.A. (2015), "An experimental and numerical study of a semi-rigid bolted-plate connections (BPC)", *J. Thin-Wall. Struct.*, **88**, 82-89.
Iftekharul, A.M. and Sabrina, F. (2015), "Numerical studies on CFRP strengthened steel columns under transverse impact", *J. Compos. Struct.*, **120**, 428-441.
Jun, D. and Marcus, M.K.L. (2007), "Behaviour under static loading of metallic beams reinforced with a bonded CFRP plate", *J. Compos. Struct.*, **78**(2), 232-242.
Jun, D., Yonghui, J. and Hengzhong, Z. (2016), "Theoretical and experimental study on notched steel beams strengthened with CFRP plate", *J. Compos. Struct.*, **136**, 450-459.
Kambiz, N., Ramli, S. and Mohd, Z.J. (2012), "Failure analysis and structural behaviour of CFRP strengthened steel I-beams", *J. Construct. Build. Mater.*, **30**, 1-9.
Karatzas, V., Kotsidis, E. and Tsouvalis, N. (2013), "An experimental and numerical study of corroded steel plates repaired with composite patches", *Proceedings of the 4th International Conference on Marine Structures, MARSTRUCT 2013*, Espoo, Finland, March.
Kotsidis, E.A., Kouloukouras, I.G. and Tsouvalis, N.G. (2014), "Finite element parametric study of a composite-to-steel-joint", In: *Maritime Technology and Engineering*, CRC Press, pp. 627-635. ISBN: 978-1-138-02727-5 (Print), 978-1-315-73159-9 (eBook), DOI: 10.1201/b17494-83.
Linghoff, D., Haghani, R. and Al-Emrani, M. (2009), "Carbon fibre composites for strengthening steel structures", *J. Thin-Wall. Struct.*, **47**(10), 1048-1058.
Maeda, T., Asano, Y., Sato, Y., Ueda, T. and Kakuta, Y. (1997), "A study on bond mechanism of carbon fiber sheet", *Proceedings of the 3rd International Symposium on Non-Metallic (FRP) Reinforcement for Concrete Structures*, (Vol. 1), Japan Concrete Institute, Sapporo, Japan, pp. 279-286.
Mohamed, E. (2014), "CFRP strengthening and rehabilitation of degraded steel welded RHS beams under combined bending and bearing", *J. Thin-Wall. Struct.*, **77**, 86-108.

Photiou, N.K., Hollaway, L.C. and Chryssanthopoulos, M.K. (2006), "Strengthening of an artificially degraded steel beam utilising a carbon/glass composite system", *J. Construct. Build. Mater.*, **20**(1), 11-21.

Pierluigi, C. and Giulia, F. (2015), "Experimental study on the fatigue behaviour of cracked steel beams repaired with CFRP plates", *J. Eng. Fract. Mech.*, **145**, 128-142.

Pouria, T.A., Saeid, S., Vaclav, K. and Habiba, B. (2015), "Investigating stress shielding spanned by biomimetic polymer-composite vs. metallic hip stem: A computational study using mechano-biochemical model", *J. Mech. Behavior Biomed. Mater.*, **41**, 51-67.

Ragheb, W.F. (2015), "Elastic local buckling of steel I-sections strengthened with bonded FRP strips", *J. Construct. Steel Res.*, **107**, 81-93.

Setvati, M.R., Zahiraniza, M., Biramarta I., Nasir, S., Zubair, I.S. and Do Kyun, K. (2016), "Meso-scale numerical study of composite patch repaired hole drilled steel plate", *ARPN J. Eng. Appl. Sci.*, **11**(3). ISSN 1819-6608

Silva, D., Lucas, F.M. and Campilho, R.D.S.G. (2012), *Advances in Numerical Modelling of Adhesive Joints*, Springer.

Stacey, A. and Birkinshaw, M. (2008), "Life extension issues for aging offshore installations", *Proceedings of the 27th International Conference on Offshore Mechanics and Arctic Engineering* (*OMAE 2008*), Estoril, Portugal, June.

Sundarraja, M.C. and Ganesh Prabhu, G. (2013), "Flexural behaviour of CFST members strengthened using CFRP Composites", *Steel Compos. Struct., Int. J.*, **15**(6), 623-643.

Tao, C., Ming Q., Xiang-Lin, G. and Qian-Qian, Y. (2015), "Flexural Strength of Carbon Fiber Reinforced Polymer Repaired Cracked Rectangular Hollow Section Steel Beams", *Journal of Polymer Science*, Article ID 204861.

Tavakkolizadeh, M. and Saadatmanesh, H. (2003), "Repair of damaged steel-concrete composite girders using carbon fiber-reinforced polymer sheets", *J. Compos. Construct.*, **7**(4), 311-322.

Teng, J.G., Fernando, D. and Yu, T. (2015), "Finite element modelling of debonding failures in steel beams flexurally strengthened with CFRP laminates", *J. Eng. Struct.*, **86**, 213-224.

Tsouvalis, N.G., Mirisiotis, L.S. and Tsiourva, T.E. (2008), "Experimental investigation of composite patch reinforced corroded steel plate in static loading", *Proceedings of the 13th European Conference on Composite Materials* (*ECCM-13*), Stockholm, Sweden, June.

Yail, J.K. and Garrett, B. (2011), "Interaction between CFRP-repair and initial damage of wide-flange steel beams subjected to three-point bending", *J. Compos. Struct.*, **93**(8), 1986-1996.

Yail, J.K. and Kent, A.H. (2010), "Modeling of steel beams strengthened with CFRP strips including bond-slip properties", *Proceedings of the CICE 2010 – The 5th International Conference on FRP Composites in Civil Engineering*, Beijing, China, September.

Yail, J.K. and Kent, A.H. (2011), "Fatigue behavior of damaged steel beams repaired with CFRP strips", *J. Eng. Struct.*, **33**(5), 1491-1502.

Yail, J.K. and Kent, A.H. (2012), "Predictive response of notched steel beams repaired with CFRP strip including bond-slip behavior", *J. Struct. Stabil. Dyn.*, **12**(1), 1-21.